

Adaptive Robust Precision Motion Control of Linear Motors with Negligible Electrical Dynamics: Theory and Experiments¹

Li Xu Bin Yao⁺

School of Mechanical Engineering
Purdue University
West Lafayette, IN 47907, USA
⁺ Email: byao@ecn.purdue.edu

Abstract

This paper studies the high performance robust motion control of linear motors that have a negligible electrical dynamics. A discontinuous projection based adaptive robust controller (ARC) is first constructed. The controller guarantees a prescribed transient performance and final tracking accuracy in general while achieving asymptotic tracking in the presence of parametric uncertainties only. A desired compensation ARC scheme is then presented, in which the regressor is calculated using desired trajectory information only. The resulting controller has several implementation advantages. Both schemes are implemented and compared on an epoxy core linear motor. Extensive comparative experimental results are presented to illustrate the effectiveness and the achievable control performance of the two ARC designs.

1 Introduction

Direct drive linear motor systems gain high-speed, high-accuracy potential by eliminating mechanical transmissions. However, they also lose the advantage of using mechanical transmissions – gear reductions reduce the effect of model uncertainties. Furthermore, certain types of linear motors are subjected to significant force ripple [1]. These uncertain nonlinearities are directly transmitted to the load and have significant effects on the motion of the load.

A great deal of effort has been devoted to solving the difficulties in controlling linear motors [1]-[5]. Alter and Tsao [2] proposed an H_∞ controller to increase dynamic stiffness for linear motor driven machine tool axes. In [3], a disturbance compensation method based on disturbance observer (DOB) [6] was proposed to make linear motors robust to model uncertainties. To reduce the effect of force ripple, in [1], feedforward compensation terms, which are based on an off-line experimentally identified model, were added to a position controller. In [4], a neural-network-based feedforward controller was proposed to reduce the effect of reproducible dis-

turbances. In [5], the idea of adaptive robust control (ARC) [7, 8] was generalized to provide a theoretic framework for the high performance motion control of linear motors.

In this paper, the proposed ARC algorithm [5] is applied on a linear motor in which the current dynamics is neglected due to the fast electric response. As pointed out in [9], however, this algorithm may have several potential implementation problems since the regressor depends on the states of the system. As a remedy, a desired compensation ARC [9, 10] in which the regressor is calculated by desired trajectory information only is then developed. The proposed controller has several implementation advantages such as reducing on-line computation time, separating the robust control design from the parameter adaptation process, reducing the effect of measurement noise, and having a faster adaptation process. Finally, comparative experimental results are presented to show the advantages and the drawbacks of each method.

2 Problem Formulation and Dynamic Models

The mathematical model of a current-controlled three-phase linear motor system is assumed to be of the form:

$$M\ddot{q} = u - F, \quad F = F_f + F_r - F_d, \quad (1)$$

where q represents the position of the inertia load, M is the inertia of the payload plus the coil assembly, u is the input voltage, F is the lumped effect of uncertain nonlinearities such as friction F_f , ripple forces F_r and external disturbance F_d . While there have been many friction models proposed [11], a simple and often adequate approach is to regard friction force as a static nonlinear function of the velocity:

$$F_f(\dot{q}) = B\dot{q} + F_{fn}(\dot{q}), \quad (2)$$

where B is the viscous friction coefficient, and F_{fn} is the nonlinear friction term which can be modeled as [11]

$$F_{fn}(\dot{q}) = -[f_c + (f_s - f_c)e^{-|\dot{q}/\dot{q}_s|^\xi}] \text{sgn}(\dot{q}), \quad (3)$$

where f_s is the level of static friction, f_c is the level of Coulomb friction, and \dot{q}_s and ξ are empirical parameters used to describe the Stribeck effect. Substituting (2) into (1) yields

$$\begin{aligned} \dot{x}_1 &= x_2, \\ M\dot{x}_2 &= u - Bx_2 - F_{fn} + \Delta, \\ y &= x_1, \end{aligned} \quad (4)$$

¹The work is supported in part by the National Science Foundation under the CAREER grant CMS-9734345 and in part by a grant from Purdue Research Foundation

where $x = [x_1, x_2]^T$ represents the position and velocity, y is the output, and $\Delta \triangleq (F_d - F_r)$ represents the lumped disturbance.

The control objective is to synthesize a control input u such that y tracks a desired trajectory $y_d(t)$ that is assumed to be second-order differentiable.

3 Adaptive Robust Control of Linear Motor Systems

3.1 Design Models and Projection Mapping

It is seen that the friction model (3) is discontinuous at $x_2 = 0$. Thus one cannot use this model for friction compensation. To by-pass this technical difficulty, a simple continuous friction model $\tilde{F}_{fn} = AS_f(x_2)$, where the amplitude A is unknown and $S_f(x_2)$ is a smooth function, will be used to approximate the actual friction model (3) for model compensation. The second equation of (4) can thus be written as:

$$M\dot{x}_2 = u - Bx_2 - AS_f + d, \quad (5)$$

where $d = \tilde{F}_{fn} - F_{fn} + \Delta$. Define an unknown parameter set $\theta = [\theta_1, \theta_2, \theta_3, \theta_4]$ as $\theta_1 = M$, $\theta_2 = B$, $\theta_3 = A$ and $\theta_4 = d_n$, where d_n is the nominal value of d . Equation (5) can thus be linearly parameterized in terms of θ as

$$\theta_1 \dot{x}_2 = u - \theta_2 x_2 - \theta_3 S_f + \theta_4 + \tilde{d}, \quad (6)$$

where $\tilde{d} = d - d_n$. For simplicity, in the following, the following notations are used: \bullet_i for the i -th component of the vector \bullet , \bullet_{\min} for the minimum value of \bullet , and \bullet_{\max} for the maximum value of \bullet . The operation $<$ for two vectors is performed in terms of the corresponding elements of the vectors. The following practical assumptions are made:

Assumption 1 The extent of the parametric uncertainties and uncertain nonlinearities are known, i.e.,

$$\theta \in \Omega_\theta \triangleq \{ \theta : \theta_{\min} < \theta < \theta_{\max} \} \quad (7)$$

$$\tilde{d} \in \Omega_d \triangleq \{ \tilde{d} : |\tilde{d}| \leq \delta_d \} \quad (8)$$

where $\theta_{\min} = [\theta_{1\min}, \dots, \theta_{4\min}]^T$, $\theta_{\max} = [\theta_{1\max}, \dots, \theta_{4\max}]^T$ and δ_d are known. \diamond

Let $\hat{\theta}$ denote the estimate of θ and $\tilde{\theta}$ the estimation error (i.e., $\tilde{\theta} = \hat{\theta} - \theta$). In view of (7), the following adaptation law with discontinuous projection modification can be used

$$\dot{\hat{\theta}} = \text{Proj}_{\hat{\theta}}(\Gamma\tau) \quad (9)$$

where $\Gamma > 0$ is a diagonal matrix, τ is an adaptation function to be synthesized later. The projection mapping $\text{Proj}_{\hat{\theta}}(\bullet) = [\text{Proj}_{\hat{\theta}_1}(\bullet_1), \dots, \text{Proj}_{\hat{\theta}_p}(\bullet_p)]^T$ is defined in [7, 12] as

$$\text{Proj}_{\hat{\theta}_i}(\bullet_i) = \begin{cases} 0 & \text{if } \hat{\theta}_i = \theta_{i\max} \text{ and } \bullet_i > 0 \\ 0 & \text{if } \hat{\theta}_i = \theta_{i\min} \text{ and } \bullet_i < 0 \\ \bullet_i & \text{otherwise} \end{cases} \quad (10)$$

It can be shown [7, 12] that for any adaptation function τ , the projection mapping used in (10) guarantees

$$\begin{aligned} \text{P1} \quad & \hat{\theta} \in \Omega_\theta \triangleq \{ \hat{\theta} : \theta_{\min} \leq \hat{\theta} \leq \theta_{\max} \} \\ \text{P2} \quad & \tilde{\theta}^T (\Gamma^{-1} \text{Proj}_{\hat{\theta}}(\Gamma\tau) - \tau) \leq 0, \quad \forall \tau \end{aligned} \quad (11)$$

3.2 ARC Controller Design

Define a switching-function-like quantity as

$$p = \dot{e} + k_1 e = x_2 - x_{2eq}, \quad x_{2eq} \triangleq \dot{y}_d - k_1 e, \quad (12)$$

where $e = y - y_d(t)$ is the output tracking error, and k_1 is any positive feedback gain. If p is small or converges to zero exponentially, then the output tracking error e will be small or converge to zero exponentially since $G_p(s) = \frac{e(s)}{p(s)} = \frac{1}{s+k_1}$ is a stable transfer function. So the rest of the design is to make p as small as possible. Differentiating (12) and substituting the expression given by (6), one obtains

$$M\dot{p} = u + \varphi^T \theta + \tilde{d} \quad (13)$$

where $\dot{x}_{2eq} \triangleq \dot{y}_d - k_1 \dot{e}$ and $\varphi^T = [-\dot{x}_{2eq}, -x_2, -S_f(x_2), 1]$. Noting the structure of (13), the following ARC control law is proposed:

$$u = u_a + u_s, \quad u_a = -\varphi^T \hat{\theta}, \quad (14)$$

where u_a is the adjustable model compensation needed for achieving perfect tracking, and u_s is a robust control law to be synthesized later. Substituting (14) into (13), and then simplifying the resulting expression, one obtains

$$M\dot{p} = u_s - \varphi^T \tilde{\theta} + \tilde{d}. \quad (15)$$

The robust control law u_s consists of two terms given by:

$$u_s = u_{s1} + u_{s2}, \quad u_{s1} = -k_2 p, \quad (16)$$

where u_{s1} is used to stabilize the nominal system, which is a simple proportional feedback with k_2 being the feedback gain in this case; u_{s2} is a robust feedback used to attenuate the effect of model uncertainties. Noting Assumption 1 and P1 of (11), there exists a u_{s2} such that the following two conditions are satisfied

$$\begin{aligned} \text{i} \quad & p\{u_{s2} - \varphi^T \tilde{\theta} + \tilde{d}\} \leq \varepsilon \\ \text{ii} \quad & pu_{s2} \leq 0 \end{aligned} \quad (17)$$

where ε is a design parameter that can be arbitrarily small. Essentially, i of (17) shows that u_{s2} is synthesized to dominate the model uncertainties coming from both $\tilde{\theta}$ and \tilde{d} ; ii of (17) is to make sure that u_{s2} is dissipating in nature so that it does not interfere with the functionality of the adaptive control part u_a . One smooth example of u_{s2} satisfying (17) is given by

$$u_{s2} = -\frac{1}{4\varepsilon} h^2 p, \quad (18)$$

where h is any smooth function satisfying $h \geq \|\theta_M\| \|\varphi\| + \delta_d$, $\theta_M = \theta_{\max} - \theta_{\min}$.

Theorem 1 Suppose that the adaptation function in (9) is chosen as $\tau = \varphi p$. Then the ARC control law (14) guarantees:

A. In general, all signals are bounded. Furthermore, a positive semi-definite function $V_s = \frac{1}{2} M p^2$ is bounded above by

$$V_s \leq \exp(-\lambda t) V_s(0) + \frac{\varepsilon}{\lambda} [1 - \exp(-\lambda t)], \quad (19)$$

where $\lambda = 2k_2/\theta_{1\max}$.

B. If after a finite time t_0 , there exist parametric uncertainties only (i.e., $\tilde{d} = 0, \forall t \geq t_0$), then, in addition to result A, zero final tracking error is achieved, i.e., $e \rightarrow 0$ and $p \rightarrow 0$ as $t \rightarrow \infty$.

Proof: The theorem can be proved in the same way as in [9].

4 Desired Compensation ARC (DCARC)

In the ARC design presented in Section 3, the regressor φ in u_a (14) and τ depends on state x . Such an adaptation structure may have several potential implementation problems [9]. Firstly, the effect of measurement noise may be severe, and a slow adaptation rate may have to be used, which in turn reduces the effect of parameter adaptation. Secondly, there may exist certain interactions between the model compensation u_a and the robust control u_s , since u_a depends on the actual feedback of the state. This may complicate the controller gain tuning process in implementation. In [13], Sadegh and Horowitz proposed a desired compensation adaptation law, in which the regressor is calculated by desired trajectory information only. The idea was then incorporated in the ARC design in [9, 10]. In the following, the desired compensation ARC will be applied on the linear motor system.

The proposed desired compensation ARC law and the adaptation law have the same forms as (14) and (9) respectively, but with the regressor φ replaced by the desired regressor φ_d :

$$u = u_a + u_s, \quad u_a = -\varphi_d^T \hat{\theta}, \quad \tau = \varphi_d p, \quad (20)$$

where $\varphi_d^T = [-\dot{y}_d, -\dot{y}_d, -S_f(\dot{y}_d), 1]$. Substituting (20) into (13), and noting $x_2 = \dot{y}_d + \dot{e}$, one obtains

$$M\dot{p} = u_s - \varphi_d^T \dot{\hat{\theta}} + (\theta_1 k_1 - \theta_2)\dot{e} + \theta_3[S_f(\dot{y}_d) - S_f(x_2)] + \ddot{d}. \quad (21)$$

Comparing (21) with (15), it can be seen that two additional terms appear, which may demand a strengthened robust control function u_s for a robust performance. Applying Mean Value Theorem, it follows that

$$S_f(x_2) - S_f(\dot{y}_d) = g(x_2, t)\dot{e}, \quad (22)$$

where $g(x_2, t)$ is a nonlinear function. The strengthened robust control function u_s has the same form as (16):

$$u_s = u_{s1} + u_{s2}, \quad u_{s1} = -k_{s1}p, \quad (23)$$

but with k_{s1} being a nonlinear gain large enough such that the matrix A defined below is positive semi-definite

$$A = \begin{bmatrix} k_{s1} - k_2 - \theta_1 k_1 + \theta_2 + \theta_3 g & -\frac{1}{2}k_1(\theta_2 + \theta_3 g) \\ -\frac{1}{2}k_1(\theta_2 + \theta_3 g) & \frac{1}{2}Mk_1^3 \end{bmatrix}. \quad (24)$$

The robust control law u_{s2} is required to satisfy the following constrains similar to (17),

$$\begin{array}{l} \text{i} \quad p\{u_{s2} - \varphi_d^T \hat{\theta} + \ddot{d}\} \leq \varepsilon \\ \text{ii} \quad pu_{s2} \leq 0 \end{array} \quad (25)$$

One smooth example of u_{s2} satisfying (25) is $u_{s2} = -\frac{1}{4\varepsilon}h_d^2 p$, where h_d is a smooth function satisfying $h_d \geq \|\theta_M\| \|\varphi_d\| + \delta_d$.

Theorem 2 *If the DCARC law (20) is applied, then*

A. *In general, all signals are bounded. Furthermore, a p.s.d. function $V_s = \frac{1}{2}Mp^2 + \frac{1}{2}Mk_1^2 e^2$ is bounded above by*

$$V_s \leq \exp(-\lambda t)V_s(0) + \frac{\varepsilon}{\lambda}[1 - \exp(-\lambda t)], \quad (26)$$

where $\lambda = \min\{2k_2/\theta_{1\max}, k_1\}$.

B. *If after a finite time t_0 , there exist parametric uncertainties only (i.e., $\ddot{d} = 0, \forall t \geq t_0$), then, in addition to result A, zero final tracking error is achieved, i.e., $e \rightarrow 0$ and $p \rightarrow 0$ as $t \rightarrow \infty$.*

Proof: The theorem can be proved in the same way as in [9].

5 Comparative Experiments

5.1 Experiment Setup

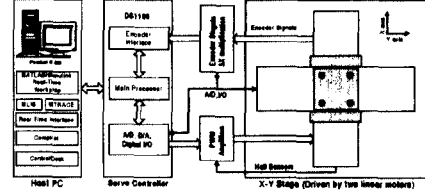


Figure 1: Experimental Setup

To test the proposed nonlinear ARC strategy and study fundamental problems associated with high performance motion control of linear motor systems, a two-axis positioning stage is set up as a test-bed. As shown in Figure 1, the test-bed consists of four major components: a precision X-Y stage with two integrated linear motors, two linear encoders, a servo controller, and a host PC. The two axes of the X-Y stage are mounted orthogonally on a horizontal plane with the Y-axis on top of the X-axis. A particular feature of the set-up is that the two linear motors are of different type: the X-axis is driven by an Anorad LCK-S-1 linear motor (iron core) and the Y-axis is driven by an Anorad LEM-S-3-S linear motor (epoxy core). The resolution of the encoders is $1\mu\text{m}$ after quadrature. The velocity signal is obtained by the difference of two consecutive position measurements. In the experiments, only Y-axis is used.

Standard least-square identification is performed to obtain the parameters of the Y-axis. The nominal values of M is $0.027(\text{V}/\text{m}/\text{s}^2)$. To test the learning capability of the proposed ARC algorithms, a 20lb load is mounted on the motor and the identified values of the parameters are

$$\theta_1 = 0.1 (\text{V}/\text{m}/\text{s}^2), \quad \theta_2 = 0.273 (\text{V}/\text{m}/\text{s}), \quad \theta_3 = 0.09 (\text{V}). \quad (27)$$

The bounds of the parameter variations are chosen as:

$$\theta_{\min} = [0.02, 0.24, 0.08, -1]^T, \quad \theta_{\max} = [0.12, 0.35, 0.12, 1]^T. \quad (28)$$

5.2 Performance Index

As in [10], the following performance indexes will be used to measure the quality of each control algorithm:

- $\|e\|_{rms} = (\frac{1}{T} \int_0^T e(t)^2 dt)^{1/2}$, the rms value of the tracking error, is used to measure *average tracking performance*, where T represents the total running time;
- $e_M = \max_t \{|e(t)|\}$, the maximum absolute value of the tracking error, is used to measure *transient performance*;
- $e_F = \max_{T-2 \leq t \leq T} \{|e(t)|\}$, the maximum absolute value of the tracking error during the last 2 seconds, is used to measure *final tracking accuracy*;

- $\|u\|_{rms} = (\frac{1}{T} \int_0^T u(t)^2 dt)^{1/2}$, the average control input, is used to evaluate the amount of *control effort*;
- $c_u = \frac{\|\Delta u\|_{rms}}{\|u\|_{rms}}$, the normalized control variations, is used to measure the *degree of control chattering*, where

$$\|\Delta u\|_{rms} = \sqrt{\frac{1}{N} \sum_{j=1}^N |u(j\Delta T) - u((j-1)\Delta T)|^2}$$

is the average of control input increments.

5.3 Comparative Experimental Results

The control system is implemented using a dSPACE DS1103 controller board. The controller executes programs at a sampling rate of $T_s = 0.4\text{ms}$, which results in a velocity measurement resolution of 0.0025m/sec . The following four controllers are compared:

PID: PID Control with Feedforward Compensation – Suppose that the parameters of (5) are known, the control objective can be achieved with the following PID control law:

$$u = \theta_1 \ddot{y}_d(t) + \theta_2 \dot{y}(t) + \theta_3 S_f(y) - K_p e - K_i \int e \, dt - K_d \dot{e}. \quad (29)$$

Closing the loop by applying (29) to (5) easily leads to the closed-loop characteristic equation

$$s^3 + \frac{K_d}{\theta_1} s^2 + \frac{K_p}{\theta_1} s + \frac{K_i}{\theta_1} = 0. \quad (30)$$

By placing the closed-loop poles at desired locations, the design parameters K_p, K_i and K_d can thus be determined. In the experiments, since θ_1, θ_2 and θ_3 are unknown parameters, instead of using (29) the following control law is applied

$$u = \hat{\theta}_1(0) \ddot{y}_d + \hat{\theta}_2(0) \dot{y} + \hat{\theta}_3(0) S_f(y) - K_p e - K_i \int e \, dt - K_d \dot{e}, \quad (31)$$

where $\hat{\theta}_1(0), \hat{\theta}_2(0)$ and $\hat{\theta}_3(0)$ are the fixed parameter estimates chosen as 0.05, 0.24 and 0.1, respectively. By placing all closed-loop poles at -300 when $\theta_1 = \theta_{1\min} = 0.02$, one obtains $K_p = 5.4 \times 10^3$, $K_i = 5.4 \times 10^5$ and $K_d = 18$.

ARC: the controller proposed in section 3. The smooth function $S_f(x_2)$ is chosen as $\frac{\pi}{2} \arctan(900x_2)$. For simplicity, in the experiments, only three parameters, θ_1, θ_3 and θ_4 , are adapted. The control gains are chosen as: $k_1 = 400, k_2 = 32$. The adaptation rates are set as $\Gamma = \text{diag}\{5, 0, 2, 1000\}$. The initial parameter estimates are: $\hat{\theta}(0) = [0.05, 0.24, 0.1, 0]^T$.

DRC: the same control law as ARC but without using parameter adaptation, i.e., letting $\Gamma = \text{diag}\{0, 0, 0, 0\}$.

DCARC: the controller proposed in section 4. The control gains are chosen as: $k_1 = 400$ and $k_{s1} = 32$. The adaptation rates are set as $\Gamma = \text{diag}\{25, 0, 5, 1000\}$.

The motor is first commanded to track a sinusoidal trajectory: $y_d = 0.05 \sin(4t)$, with a 20lb load mounted on the motor (The inertia is equivalent to $M = 0.1$). The experimental results in terms of performance indexes are given in table 1. As seen from the table, in terms of e_M, e_F and $\|e\|_{rms}$, PID performs poorly but with a slightly less degree of control input chattering. One may argue that the performance of PID control can be further improved by increasing the feedback

gains. However, in practice, feedback gains have upper limits because the bandwidth of every physical system is finite. To verify this claim, the closed-loop poles of the PID controller are placed at -320 instead of -300 , which is easily translated into $K_p = 6144, K_i = 655360$ and $K_d = 19.2$. With these gains, the closed-loop system is found to be unstable in experiments. This indicates that the closed-loop bandwidth that a PID controller can achieve in implementation has been pushed almost to its limit and not much further performance improvement can be expected from PID controllers. Thus, in order to realize the high performance potential of the linear motor system, a PID controller even with feedforward compensation may not be sufficient.

| controller | PID | DRC | ARC | DCARC |
|---------------------------------|------|------|------|-------|
| e_M (μm) | 156 | 56.3 | 36.1 | 30.4 |
| e_F (μm) | 21.2 | 11.2 | 5.1 | 5.1 |
| $\ e\ _{rms}$ (μm) | 8.04 | 5.07 | 1.99 | 1.78 |
| $\ u\ _{rms}$ (V) | 0.20 | 0.19 | 0.19 | 0.19 |
| $\ \Delta u\ _{rms}$ (V) | 0.06 | 0.10 | 0.12 | 0.09 |
| c_u | 0.28 | 0.56 | 0.66 | 0.47 |

Table 1

The tracking errors are given in Figure 2 (the tracking error of the PID controller is chopped off). If one compares ARC with DCARC, it is seen that ARC has a relatively poor transient tracking performance. The reason is that only slower adaptation rate can be used for ARC, which reduces the effect of parameter adaptation. When we tried to increase the adaptation rate for ARC further, the system is subjected to quite severe control chattering due to the measurement noises (especially velocity feedback). Comparatively, due to the use of desired compensation structure, DCARC is not so sensitive to velocity measurement noise. In return, a larger adaptation rate can be used and the parameter adaptation algorithm of DCARC is able to pick up the actual value of the inertial load more quickly.

To test the performance robustness of the algorithms to parameter variations, the 20lb payload is removed, which is equivalent to $M = 0.027$. The tracking errors are given in Figure 3. It shows that both ARC and DCARC achieve good tracking performance in spite of the change of inertia load.

Finally, the controllers are test for tracking a fast point-to-point motion trajectory shown in Figure 4. The trajectory has a maximum velocity of $v_{\max} = 1\text{m/s}$ and a maximum acceleration of $a_{\max} = 12\text{m/s}^2$. The tracking errors are shown in Figure 5. As seen, the proposed DCARC has a much better performance than PID and DRC. Furthermore, during the zero velocity portion of motion, the tracking error is within $\pm 1\mu\text{m}$.

6 Conclusions

In this paper, an ARC controller and a desired compensation ARC controller have been developed for high performance robust motion control of linear motors. The proposed controllers take into account the effect of model uncertain-

ties coming from the inertia load, friction force, force ripple and external disturbances. The resulting controllers guarantee a prescribed transient performance and final tracking accuracy in general while achieving asymptotic tracking in the presence of parametric uncertainties only. Furthermore, it is shown that the desired compensation ARC scheme, in which the regressor is calculated using desired trajectory information only, offers several implementation advantages such as less on-line computation time, reduced effect of measurement noise, a separation of the robust control design from the parameter adaptation, and a faster adaptation rate in implementation. Experimental results illustrate the high performance of the proposed ARC strategies and show the advantages and drawbacks of each method.

References

- [1] P. V. Braembussche, J. Swevers, H. V. Brussel, and P. Vanherck, "Accurate tracking control of linear synchronous motor machine tool axes," *Mechatronics*, vol. 6, no. 5, pp. 507–521, 1996.
- [2] D. M. Alter and T. C. Tsao, "Control of linear motors for machine tool feed drives: design and implementation of H_∞ optimal feedback control," *ASME J. of Dynamic Systems, Measurement, and Control*, vol. 118, pp. 649–656, 1996.
- [3] T. Egami and T. Tsuchiya, "Disturbance suppression control with preview action of linear dc brushless motor," *IEEE Transactions on Industrial Electronics*, vol. 42, no. 5, pp. 494–500, 1995.
- [4] G. Otten, T. Vries, J. Amerongen, A. Rankers, and E. Gaal, "Linear motor motion control using a learning feedforward controller," *IEEE/ASME Transactions on Mechatronics*, vol. 2, no. 3, pp. 179–187, 1997.
- [5] B. Yao and L. Xu, "Adaptive robust control of linear motor for precision manufacturing," in *Proc. IFAC'99 World Congress*, vol. A, pp. 25–30, 1999.
- [6] S. Komada, M. Ishida, K. Ohnishi, and T. Hori, "Disturbance observer-based motion control of direct drive motors," *IEEE Transactions on Energy Conversion*, vol. 6, no. 3, pp. 553–559, 1991.
- [7] B. Yao and M. Tomizuka, "Smooth robust adaptive sliding mode control of manipulators with guaranteed transient performance," *Trans. of ASME, Journal of Dynamic Systems, Measurement and Control*, vol. 118, no. 4, pp. 764–775, 1996.
- [8] B. Yao and M. Tomizuka, "Adaptive robust control of siso nonlinear systems in a semi-strict feedback form," *Automatica*, vol. 33, no. 5, pp. 893–900, 1997.
- [9] B. Yao, "Desired compensation adaptive robust control," in *ASME International Mechanical Engineering Congress and Exposition (IMECE'98), DSC-Vol.64*, pp. 569–575, 1998.
- [10] B. Yao and M. Tomizuka, "Comparative experiments of robust and adaptive control with new robust adaptive controllers for robot manipulators," in *Proc. of IEEE Conf. on Decision and Control*, pp. 1290–1295, 1994.
- [11] B. Armstrong-Hélouvry, P. Dupont, and C. Canudas de Wit, "A survey of models, analysis tools and compensation methods for the control of machines with friction," *Automatica*, vol. 30, no. 7, pp. 1083–1138, 1994.
- [12] S. Sastry and M. Bodson, *Adaptive Control: Stability, Convergence and Robustness*. Englewood Cliffs, NJ 07632, USA: Prentice Hall, Inc., 1989.
- [13] N. Sadegh and R. Horowitz, "Stability and robustness analysis of a class of adaptive controllers for robot manipulators," *Int. J. Robotic Research*, vol. 9, no. 3, pp. 74–92, 1990.

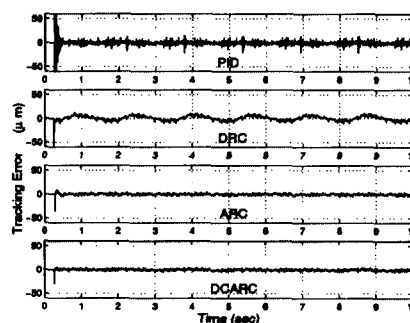


Figure 2: Tracking errors for sinusoidal trajectory with load

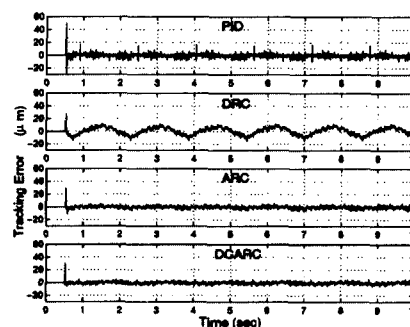


Figure 3: Tracking errors for sinusoidal trajectory without load

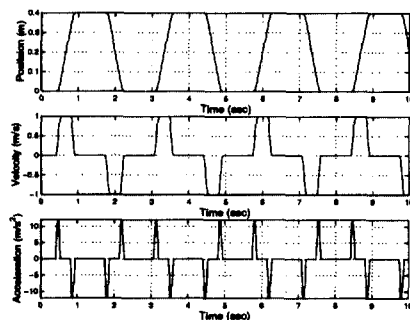


Figure 4: Point-to-point motion trajectory

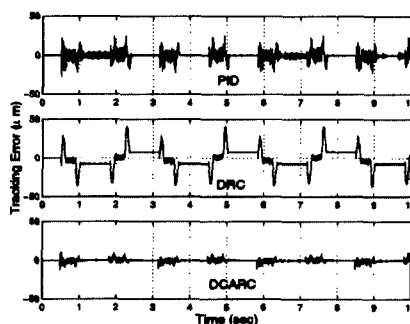


Figure 5: Tracking errors for the point-to-point motion trajectory